

Structure-property relations in non-linear, segmented copolyureas formed by reaction injection moulding, RIM

A. J. Ryan*, J. L. Stanford, and A. N. Wilkinson

Department of Polymer Science and Technology, University of Manchester, Manchester M60 1QD, England

Summary

Segmented copolyureas have been formed by RIM using a MDI-based polyisocyanate (RMA400) and mixtures of a polyether triamine (Jeffamine T5000) and diethyltoluene diamine (DETDA) chain extender. Hard segment (HS) content was varied between 35 and 65% w/w at a constant overall stoichiometric ratio of $-NCO$ to $-NH_2$ groups of 1.03. All the copolyureas were translucent and DSC confirmed their totally amorphous structure.

The copolyureas were shown by dynamic mechanical-thermal analysis to possess a two-phase morphology comprising polyether soft segments of constant T_g^S of $-40^\circ C$ and aromatic polyurea hard segments with T_g^H increasing from 215 to $236^\circ C$ as HS content increased. The ratio of flexural moduli at -35 and $65^\circ C$, decreased from 4.9 to 2.2 at 65% HS, and mechanical integrity was retained at temperatures in excess of $250^\circ C$, with flexural moduli of 10MPa at $270^\circ C$.

Tensile stress-strain studies showed the polyureas to range from semi-rigid elastomers to stiff plastics with moduli greater than 1GPa. Postcuring significantly improves materials toughness at high HS contents.

Introduction

Polyureas formed by reaction injection moulding offer distinct advantages in terms of processing and superior physical and mechanical-thermal properties, when compared with polyurethane and poly(urethane-urea) counterparts (1-6). The RIM-polyureas are segmented copolymers formed from mixtures of amine-functionalised, polyether pre-polymers and hindered diamine chain extenders, reacted with polyisocyanates. The intrinsically fast amine-isocyanate reaction enables short cycle times ($\sim 10s$) to be achieved (1,4) without the use of catalysts, which in turn allows internal mould release agents such as carboxy-functional siloxanes and zinc stearate to be used directly (2,5). In addition, postcuring of RIM-polyureas has been shown to be unnecessary (3), provided that RIM-mould temperatures are sufficiently high ($\sim 140^\circ C$).

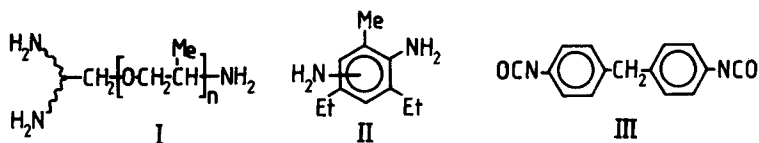
Previous work reported on non-linear polyureas (1-5) has not included dynamic mechanical-thermal data, and the only systematic study on structure-property relations of RIM-polyureas to include such data has been restricted to a linear system at only one hard segment level (6). This paper presents preliminary results of systematic studies on non-linear, segmented copolyureas and correlates the dynamic mechanical-thermal and tensile stress-strain behaviour of such RIM-materials containing different hard segment contents.

* To whom offprint requests should be sent

Experimental

Reactants.

The reactants used, whose structures are shown below, were a polyamine (I), a hindered-diamine chain extender (II) and a polyisocyanate based on 4,4'-methylenediphenylene diisocyanate, MDI (III). The polyamine, Jeffamine T5000 (ex. Texaco Chemicals), was a polyoxypropylene triamine with a nominal molar mass of 5,000g/mol. The chain extender,



3,5-diethyltoluene diamine DETDA (ex. Lonza AG), was an 80:20 mixture of 2,4- and 2,6-isomers. The polyisocyanate, Isonate RMA400 (ex. UpJohn/Dow), had an equivalent weight of 160g/mol by end-group analysis (7).

Reaction Injection Moulding.

Polyureas were moulded as rectangular plaques (700 x 400 x 3mm) using in-house RIM equipment which has been described in detail elsewhere (8). The overall stoichiometric ratio, defined as the ratio of isocyanate to total amine groups, was kept constant at 1.03. Hard segment content was increased from 35 to 65% w/w by increasing the ratio of DETDA to T5000 in the polyamine/diamine reactant mixture. A constant machine throughput of 500g/s was used for the polyamine/diamine reactant stream and the corresponding throughputs of the polyisocyanate reactant stream were increased from 200 to 425g/s so as to maintain the reactant stoichiometry. Initial reactant and RIM-mould temperatures of 35 and 117°C, respectively, were used throughout, and typical gel times were of the order of 2 seconds with mould filling occurring in about 1 second.

Characterisation of RIM-Polyureas.

Non-postcured and postcured (100°C/18h) materials were characterised using DSC, dynamic mechanical thermal analysis (DMTA) and tensile stress-strain measurements. DSC measurements were made on a Dupont 990 Thermal Analyser equipped with a DSC cell. Samples (~10mg) and an inert reference material, glass beads (~10mg), were encapsulated in aluminium pans and cooled to -120°C in the cell which was then heated at 20°C/min in air to 350°C. Glass transition temperatures and corresponding heat capacity changes per unit sample mass, $\Delta C_p/m$, were determined from DSC traces as previously described (7). DMTA data were obtained at a frequency of 1Hz in the temperature range -100 to 300°C at a heating rate of 5°C/min. A double-cantilever bending geometry was used for beam samples (3 x 10 x 45mm) to obtain dynamic flexural modulus and mechanical damping as functions of temperature. Tensile stress-strain data (ASTM D638M-81) were obtained at 23°C on an Instron 1122 Universal Testing Machine using dumb-bell specimens deformed at an extension rate of 10mm/min.

Results and Discussion

The properties of the RIM-polyureas are dominated, as expected, by the essentially two-phase structure comprising urea end-linked, polyether soft segments and rigid, extensively-hydrogen bonded, DETDA/MDI-based hard segments. During the RIM-process, the much faster rate of reaction of -NCO

groups toward the aliphatic, polyether $-NH_2$ groups, compared with those of the aromatic DETDA, results in the rapid formation of $-NCO$ -tipped T5000 oligomers whose mean molar mass is low due to the large excess of RMA400 to T5000 present in the initial polymerisation stages. Consecutive-competitive reaction between DETDA and RMA400 then produces incompatible hard segments which, depending on molar mass, undergo vitrification. Simultaneously, an essentially star block copolymer structure develops from further reactions between $-NCO$ -tipped T5000 oligomers, DETDA and $-NH_2$ -tipped, DETDA/MDI hard segments, leading eventually to gross-gelation/vitrification and ultimate formation of a heterogeneous macro-network with well developed connectivity between hard and soft segment phases. These phenomena occur to varying degrees and at different stages in the overall polymerisation depending on hard segment content and associated adiabatic temperature conditions generated during the RIM-process.

Dynamic Mechanical Thermal Analysis.

Table 1 summarises the essential dynamic properties derived from the median DMTA plots of figures 1 and 2. Overall, two major transitions are observed, namely, soft segment and hard segment glass transitions occurring, respectively, at temperatures Tg^S ($\sim -40^\circ C$) and Tg^H (210 to $240^\circ C$). (Similar transitional behaviour was obtained from loss modulus, E'' , versus temperature plots which showed corresponding Tg^S -peaks about $5^\circ C$ lower and with the exception of UD35, Tg^H -peaks, about $35^\circ C$ lower than the respective temperatures reported in Table 1.) A third, less intense and broader transition observed between 50 and $100^\circ C$, is attributed to co-operative molecular relaxations of mixed soft and hard segments. A fourth transition, evident as a shoulder between 130 and $190^\circ C$ on the Tg^H -peak for UD35, is ascribed to secondary molecular relaxations of lower molar mass polyurea oligomers in the hard segment phase. This shoulder is barely discernible in UD50 and completely absent in UD65 as the mean molar mass of the hard segments increases.

The value of Tg^S is independent of HS content as reported previously (7) for corresponding diamine chain extended, RIM-copoly(urethane-urea)s.

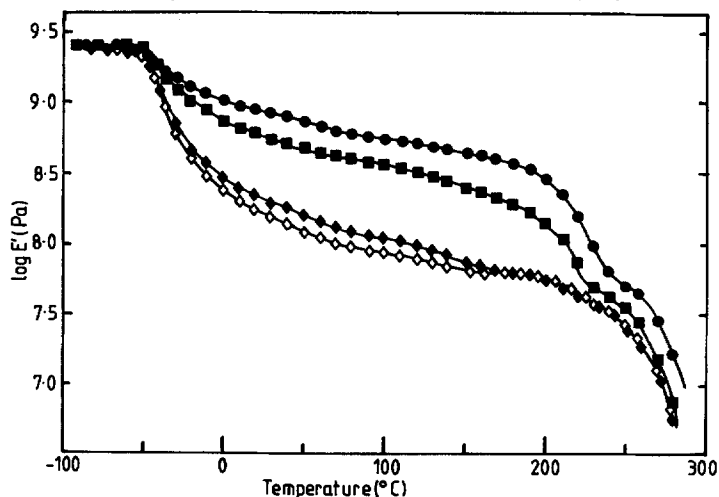


Figure 1. Dynamic flexural modulus (E') versus temperature for postcured segmented copolyureas with different hard segments contents. UD35 \blacklozenge ; \blacksquare UD50; \bullet UD65. Data for non-postcured UD35 \diamond are also included.

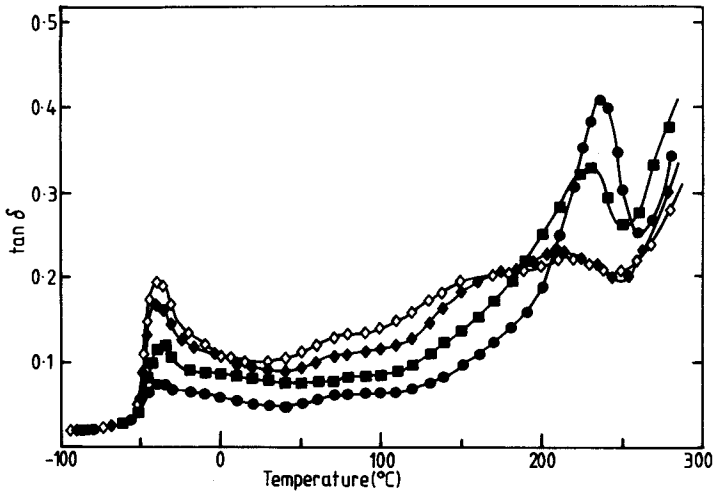


Figure 2. Mechanical damping ($\tan\delta$) versus temperature for postcured segmented copolyureas. Key as for figure 1.

However, T_g^H is shown to rise with HS content, with the largest increase from 215 to 230°C between 35 and 50% HS being due possibly to a marked increase in hard segment length in this composition region. The adiabatic temperature rise produced in the UD35 system is much less than for UD50 or UD65, which causes vitrification to occur earlier in the polymerisation and inhibits development of high hard segment molar mass. Table 1 also shows values of $\tan\delta$ associated with each T_g^S and T_g^H transition, and the peak intensities are seen to decrease and increase, respectively in direct proportion to the weight fractions of soft and hard segments.

The modulus ratio values, $E'(-30^\circ\text{C})/E'(65^\circ\text{C})$, for postcured polyureas decrease significantly with increasing HS content, due mainly to the values of E' at -30°C , a temperature which is close to T_g^S for all materials. Clearly the magnitude of the modulus drop in the T_g^S region decreases with increasing HS content whilst at 65°C , the rate of change of E' with temperature is essentially constant. The modulus-temperature dependence at elevated temperatures is shown over an equal temperature interval (95°C) in Table 1 by the modulus ratio values $E'(65^\circ\text{C})/E'(160^\circ\text{C})$ which when compared with the $E'(-30^\circ\text{C})/E'(65^\circ\text{C})$ ratios, are not only lower but also show a much smaller dependence on HS content. The $E'(65^\circ\text{C})/E'(160^\circ\text{C})$ ratios illustrate quite clearly the superior and prolonged, high-temperature dimensional stability of RIM-polyureas over corresponding poly(urethane-urea)s (7) and polyurethanes (8,9). In fact, even at 250°C , the polyureas still retain significant mechanical integrity with moduli between 20 and 50MPa.

Table 1. DMTA for RIM-Copolyureas

Polyurea	T_g^S		T_g^H		$\frac{E'(-30^\circ\text{C})}{E'(65^\circ\text{C})}$	$\frac{E'(65^\circ\text{C})}{E(160^\circ\text{C})}$
	$^\circ\text{C}$	$\tan\delta$	$^\circ\text{C}$	$\tan\delta$		
UD35npc	-39	0.19	215	0.23	5.6	1.8
UD35pc	-38	0.18	215	0.24	4.9	2.0
UD50pc	-38	0.12	230	0.33	2.9	1.8
UD65pc	-40	0.08	236	0.41	2.2	1.5

npc non-postcured; pc postcured

Comparison of UD35npc and UD35pc shows that postcuring has little effect on the values of T_g^S and T_g^H , but does reduce the level of damping (and increases modulus) in the inter-transitional region between 0 and 160°C. The $E'(-30^\circ\text{C})/E'(65^\circ\text{C})$ ratio is reduced from 5.6 to 4.9 due mainly to the increased value of E' at 65°C brought about by postcuring which completes chemical reaction in the RIM-polyureas and modifies morphology by an annealing process. At the post-curing temperature (100°C), the molecular mobility of the soft segment phase allows any isolated HS present prior to postcuring to associate itself closer to the HS phase and also enables the boundaries between the phases to become more distinct.

Differential Scanning Calorimetry (DSC).

The DSC data summarised in Table 2 were derived from DSC traces which were essentially featureless, showing only a broad soft segment glass transition around -60°C and exothermic behaviour at about 300°C resulting from thermal degradation. Although hard segment glass transitions were not observed, the absence of any melting endotherms confirms the totally amorphous structure of the copolyureas. The T_g^S endotherms extend over a 30°C range and the T_g^S -values in Table 2 were determined at the onset of the endothermic change in base-lines of DSC traces, which accounts for the lower values compared with T_g^S reported in Table 1. T_g^S for T5000 (-64°C) is raised by about 5°C in the polyureas which is typical of the increase expected for similar end-linked polyethers (10). In these polyureas the degree of phase separation, between 60 and 64%, see Table 2, is shown as a plot of $\Delta C_p/m$ in figure 3, in which the solid and dashed lines represent complete (100%) and partial (65%) phase separation, respectively. Figure 3, therefore shows the polyureas to be slightly more phase-mixed compared with corresponding poly(urethane-urea)s reported previously(7). This is a consequence of the much higher reactivity of the soft segment oligomer in these polyurea forming systems.

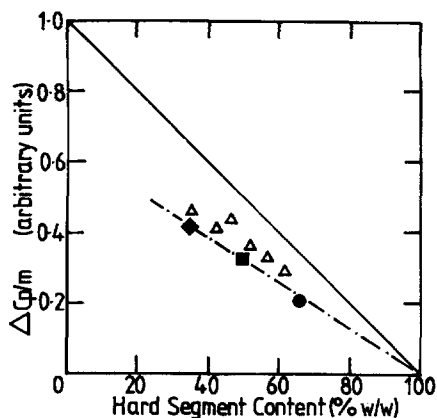


Table 2. Transitional and Phase Separation Behaviour (DSC) of Copolyureas.

Polyurea	T_g (°C)	$\Delta C_p/m$	Phase Separation (%)
UD35pc	-58	0.41	63
UD50pc	-58	0.32	64
UD65pc	-59	0.21	60
T5000	-64	1.00	-

Figure 3. The variation of $\Delta C_p/m$ with hard segment content for segmented copolyureas compared with corresponding segmented copoly(urethane-urea)s (7). Closed symbols, copolyureas; open triangles, copoly(urethane-urea)s.

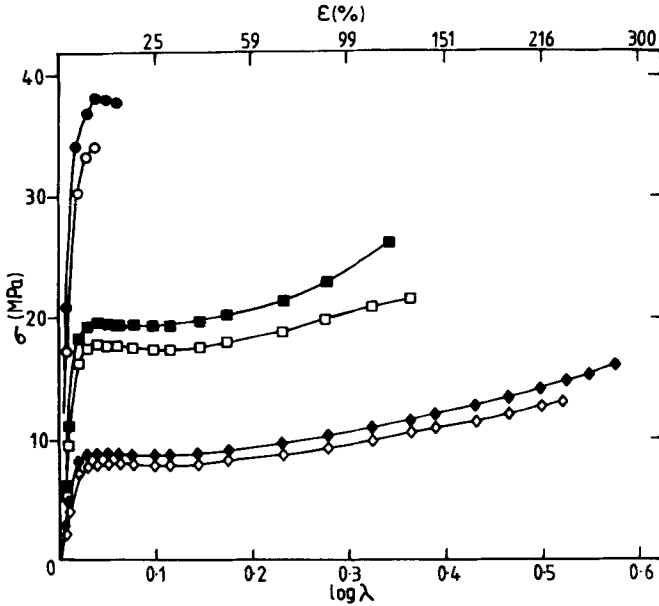


Figure 4 Tensile stress-strain curves for segmented copolyureas showing the effects of hard segment content and postcuring. λ is the extension ratio. Open symbols, non-postcured; closed symbols, postcured. UD35 \diamond , \blacklozenge ; UD50 \square , \blacksquare ; UD65 \circ , \bullet .

Tensile Stress-Strain.

The RIM-polyureas were all translucent materials, ranging in physical behaviour from flexible elastomers (UD35) to rigid plastics (UD65). Tensile stress-strain curves are shown in figure 4 and derived tensile properties are summarised in Table 3: all curves and properties are the mean of at least 5 determinations. As HS content increases, modulus (E) increases four-fold and tensile strength (σ_u) is more than doubled, but elongation (ϵ_u) decreases by an order of magnitude. All the postcured materials exhibit a yield point (see σ_y and ϵ_y in Table 3) with the amount of post-yield drawing decreasing markedly as HS content increases. Despite the large increases in stiffness and strength the overall effect of HS content therefore, is to reduce material tensile toughness, U_t determined as the integrated area under a stress-strain curve, as shown by the values in Table 3. Postcuring generally improves tensile properties and appears to be particularly important for high HS content materials (UD65) for which

Table 3. Tensile Stress-Strain Properties (23°C) of RIM Copolyureas

Polyurea	E (MPa)	σ_y (MPa)	ϵ_y (%)	σ_u (MPa)	ϵ_u (%)	U_t (MJm ⁻³)
UD35npc	221	8.1	14	13.1	232	35.1
UD35pc	276	8.9	10	15.9	276	48.5
UD50npc	504	17.8	13	22.4	133	37.4
UD50pc	617	19.6	13	25.0	119	38.4
UD65npc	951	-	-	34.2	9	3.5
UD65pc	1144	38.4	11	37.6	17	8.6

the value of U_t is more than doubled. Thus, the brittle, non-yielding UD65npc is transformed by postcuring into a rigid, semi-ductile material which, as can be seen in figure 4, shows a small but nonetheless distinct yield point. Previous studies (11) reported the structure of similar RIM-copoly(urethane-urea)s to comprise a continuous-dispersed, two-phase morphology with phase inversion occurring at about 55% HS. Such a morphology might not exist in the copolyureas because of the mode of polymerisation occurring during the RIM-process, described earlier, is more likely to result in the formation of a bi-continuous, two-phase morphological structure (12) in these materials. To determine such a morphology requires further studies, currently in progress, on a wider range of RIM-copolyureas.

Acknowledgements

The authors would like to thank Dr. R.J.G. Dominguez of the Texaco Chemical Company for the kind donation of the polyether triamine, Jeffamine T5000.

References

1. Dominguez, R.J.G., J.Cell.Plast. 20, 433 (1984).
2. Grigsby, R.A., Dominguez, R.J.G., Proc. SPI 29th Am.Tech. & Mark.Conf., Nevada, October 1985.
3. Ewen, J.H., J.Elast.Plast. 17, 281(1985).
4. Vespoli, H.P., Alberino, L.M., Peterson, A.A., Ewen, J.H., J.Elast.Plast. 18, 159 (1986).
5. Grigsby, R.A., Rice, D.M., J.Cell.Plast. 22, 484 (1986).
6. Camargo, R.E., Andrews, J.S., Macosko, C.W., Wellinghoff, S.T., Polym.Prep. 25(2), 294 (1984).
7. Ryan, A.J., Stanford, J.L., Still, R.H., Br.Polym.J. *in press* (1987).
8. Barksby, J., Dunn, D., Kaye, A., Stanford, J.L., Stepto, R.F.T., in "Reaction Injection Moulding," ed. by J.E. Kresta, ACS Symp.Ser. 270, ACS Washington DC, 83 (1985).
9. Camargo, R.E., Macosko, C.W., Tirrell, M., Wellinghoff, S.T., in "Reaction Injection Moulding," ed. by J.E. Kresta, ACS Symp.Ser. 270, ACS, Washington DC, 27 (1985).
10. Camberlin, Y., Pascault, J.P., J.Polym.Sci. (Polym.Chem.Ed.) 27, 415 (1983).
11. Ryan, A.J., Stanford, J.L., Still, R.H., in "Integration of Fundamental Polymer Science and Technology, II" ed. by L.A. Kleintjens and P.J. Lemstra, *in press* (1987).
12. Thomas, E.L. *private communication*.

Accepted October 15, 1987 C